



# Upgrade of nickel and iron from low-grade nickel laterite by improving direct reduction-magnetic separation process

Hong-yu Tian<sup>1</sup> · Zheng-qi Guo<sup>1</sup> · Ruo-ning Zhan<sup>1</sup> · Jian Pan<sup>1</sup> · De-qing Zhu<sup>1</sup> · Cong-cong Yang<sup>1</sup> · Liao-ting Pan<sup>2</sup> · Xue-zhong Huang<sup>2</sup>

Received: 12 April 2021 / Revised: 5 June 2021 / Accepted: 5 June 2021 / Published online: 23 August 2021  
© China Iron and Steel Research Institute Group 2021

## Abstract

Low-grade saprolite nickel laterite, characterized by complicated minerals composition and fine-grained and complex dissemination, was commonly treated with a low recovery efficiency of Ni and Fe by conventional methods. Hence, an improved direct reduction and magnetic separation process was proposed. Meanwhile, the mechanisms on the enhanced growth of the Ni–Fe particles and the phase transformation in the nickel laterite pellets were explored. The low-nickel concentrates as a nucleating agent can obviously decrease the activation energy for growth of Ni–Fe alloy particles during the improved direct reduction process from 197.10 to 154.81 kJ/mol when the low-nickel concentrates were added from 0 to 20%. Hence, it is able to decrease nucleation barrier, induce the growth of Fe–Ni alloy particles and increase their average size. As a result, the size of Ni–Fe particles in the pellets from less than 10 μm grew to more than 20 μm, which is beneficial for the full liberation and recovery of Ni and Fe in subsequent magnetic separation process. Therefore, the preferable Ni–Fe alloy concentrates with 6.44% Ni and 82.48% Fe can be prepared with corresponding recovery rates of 96.90% and 95.92%, respectively, when adding 20% low-nickel concentrates.

**Keywords** Nickel laterite · Low-nickel concentrate · Nucleating agent · Growth kinetics · Ni–Fe alloy · Direct reduction · Magnetic separation

## 1 Introduction

Nickel as an important metallic element in the stainless steel has an increasing demand in recent years [1]. The nickel laterite and nickel sulfide ores are both the main land-based nickel resources, and the former accounts for up to 72% of the world's nickel reserves and is in connection with nearly 40% of the global nickel production. However, with the depletion of easy-to-use nickel sulfide ore, the sharp attention and extensive utilization of nickel laterite will gradually become mainstream for the extraction of

nickel [2, 3]. As previous studies reported, nickel is mainly present as oxide and silicate in the nickel laterite with corresponding existence in the form of adsorbed state to combine with goethite and ionic exchange to replace magnesium of serpentine, respectively, which indicates that the nickel laterite is difficult to be treated effectively by physical mineral processing technologies [4, 5]. Hence, many studies, involving pyrometallurgical and hydrometallurgical processes, have been conducted for the concentration of nickel from nickel laterite [6–9]. In consideration of the main application field and potential production cost of nickel, compared with the electrolytic nickel mainly produced from hydrometallurgical processes, the ferrometal produced from pyrometallurgical processes, as the raw material of argon oxygen decarburization (AOD) furnace for stainless steel, has an obvious cost advantage by avoiding the prior separation of nickel and iron before high temperature fusion [10, 11].

At present, rotary kiln-electric furnace (RKEF) characterized by large scale of production and good quality of

✉ Zheng-qi Guo  
guozqcsu@csu.edu.cn

✉ Jian Pan  
pjcsu@csu.edu.cn

<sup>1</sup> School of Minerals Processing and Bioengineering, Central South University, Changsha 410083, Hunan, China

<sup>2</sup> Beibu Gulf New Materials Co., Ltd.,  
Beihai 536000, Guangxi, China

product is still the main pyrometallurgical process to produce crude ferronickel from saprolite laterite ore [12, 13]. However, affected by supply–demand relationship and export policy of nickel-rich country in reserves, with the decrease in nickel grade below 1.6 wt.% and the increase in Fe/Ni above 10 in the imported low-grade nickel laterite, the higher energy consumption of RKEF process for per ton nickel of ferronickel is unavoidable, which limits the economic benefit to some extent [14, 15]. Owing to this situation, the direct reduction and magnetic separation, as a significant pyrometallurgical process with obvious superiority of compact process flow route, low energy consumption and controllable environmental influence, gradually becomes one of the alternative options to effectively upgrade the nickel from low-grade nickel laterite [16, 17]. However, low-grade nickel laterite with complicated minerals composition, fine-grained dissemination and high content of gangue elements commonly has a low recovery of nickel and iron. It is because not only the nickel(iron)-bearing phases are difficult to be reduced to metallic states, but also the reduced ferronickel particles are too fine to migrate, aggregate and grow during the reduction stage, which is hard to full liberation in subsequent magnetic separation [17–21]. According to the studies reported, in order to improve the recycling efficiency of nickel and iron from nickel laterite, the common effective methods mainly including the optimization of reduction conditions and addition of suitable additives were recommended [22, 23]. The high reduction temperature and addition of additives (such as sulfides, alkali salts, chlorides and fluxes) can not only destroy the lattice structure of silicate minerals to release the nickel (iron)-bearing phases, but also generate suitable quantity of liquid phases to enhance the mass transfer effects, resulting in a sufficient reduction, migration, aggregation and growth of ferronickel particles [24, 25]. The sufficient size of ferronickel particles ( $\geq 20 \mu\text{m}$ ) generated in the stage of direct reduction is crucial to meet the requirement of subsequent magnetic separation, which is beneficial to saving energy consumption for fine grinding reduced ores and improving recycling of nickel [26]. However, the enhanced methods with elevated temperature up to at least 1300 °C or high additive dosage (about 8%–20%) for effective treatment of low-grade nickel laterite via the direct reduction and magnetic separation process are also

unavoidable to be taken into consideration, which will inevitably increase the cost of production and decrease life span of equipment [27, 28]. Hence, it is significant to improve the size of ferronickel particles and recycling efficiency of nickel in an effective and economical way. Some researchers have tried to use high iron-bearing mineral powders (such as iron ore concentrates and limonitic laterite ore) as nucleating agents for the growth of ferronickel particles, which can contribute to the recycling of nickel from low-grade nickel laterite [29, 30], but it is difficult to obtain the products with high-grade nickel because of the high Fe/Ni of nucleating agents.

In this study, an improved direct reduction and magnetic separation process was proposed by addition of low-nickel concentrates as nucleating agent combined with low quantity of composite additive to upgrade the nickel and iron from low-grade nickel laterite. The corresponding enhancing mechanism of synergistic effects between nucleating agent and composite additive as well as the growth behavior of ferronickel fine particles was also disclosed.

## 2 Experimental

### 2.1 Materials

#### 2.1.1 Nickel laterite ore

The chemical composition of nickel laterite as received from Philippines employed in the study is shown in Table 1. It indicates that the nickel laterite contains 1.29 wt.% Ni, 16.31 wt.% Fe, 32.28 wt.% SiO<sub>2</sub> and 27.38 wt.% MgO with both high Fe/Ni of 12.64 and MgO/SiO<sub>2</sub> of 0.85, while the impurity elements, such as S and P, remain at an extremely low level of 0.002 and 0.003 wt.%, respectively. The phase composition of nickel laterite can be analyzed by X-ray diffraction (XRD) pattern as shown in Fig. 1, which verified that the lizardite is the major mineral phase of nickel laterite, and meanwhile, clinocllore, quartz, goethite and hematite as the minor mineral phases can also be detected. It can thus be seen that the nickel laterite is a typical low-grade saprolite laterite.

The microstructure of nickel laterite and the occurrence characteristics of nickel can be revealed by scanning

**Table 1** Chemical compositions of nickel laterite (wt.%)

TNi	TFe	MgO	SiO <sub>2</sub>	Al <sub>2</sub> O <sub>3</sub>	CaO	Cr <sub>2</sub> O <sub>3</sub>	S	P	LOI
1.29	16.31	27.38	32.28	1.74	0.36	1.32	0.002	0.003	7.88

LOI Loss on ignition

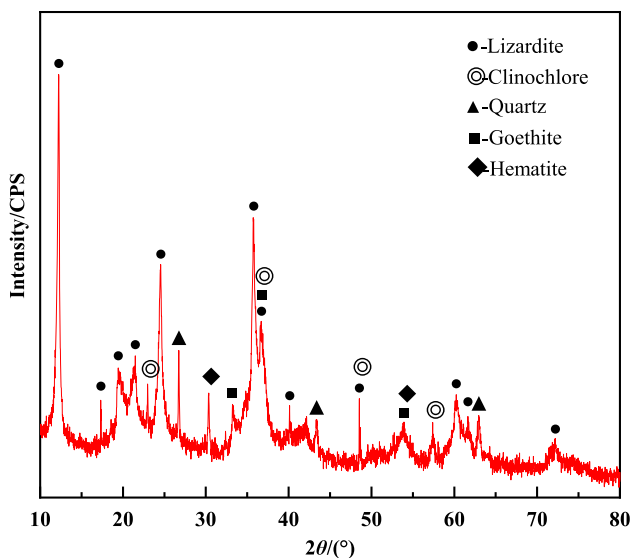


Fig. 1 XRD pattern of nickel laterite

electron microscopy combined with energy dispersive spectrometry (SEM–EDS) patterns as shown in Fig. 2. It indicates that the nickel-bearing phases, such as lizardite,

clinoclhore and goethite, show close symbiotic relations with each other, which has a negative effect on the reduction in nickel(iron)-bearing phases and the growth of reduced Ni–Fe particles for meeting the requirement of subsequent magnetic separation from gangue minerals.

### 2.1.2 Reductant

A soft coal was used as the reductant in this study. The particle size of soft coal is less than 1.0 mm (80% passing 0.074 mm). The proximate and fusibility analyses of reductant and chemical composition of ash were detected referring to the Chinese standards GB/T212-2008, GB/T219-2008 and GB/T31391-2015, and the results are summarized in Tables 2 and 3, respectively. It indicates that the soft coal has not only a high level of fixed carbon and volatile matter with a suitable ash content, but also a good ash fusibility. Furthermore, the content of sulfur in the ash is also low enough. The characteristics of soft coal can completely satisfy the requirement of reductant for the reduction in nickel laterite.

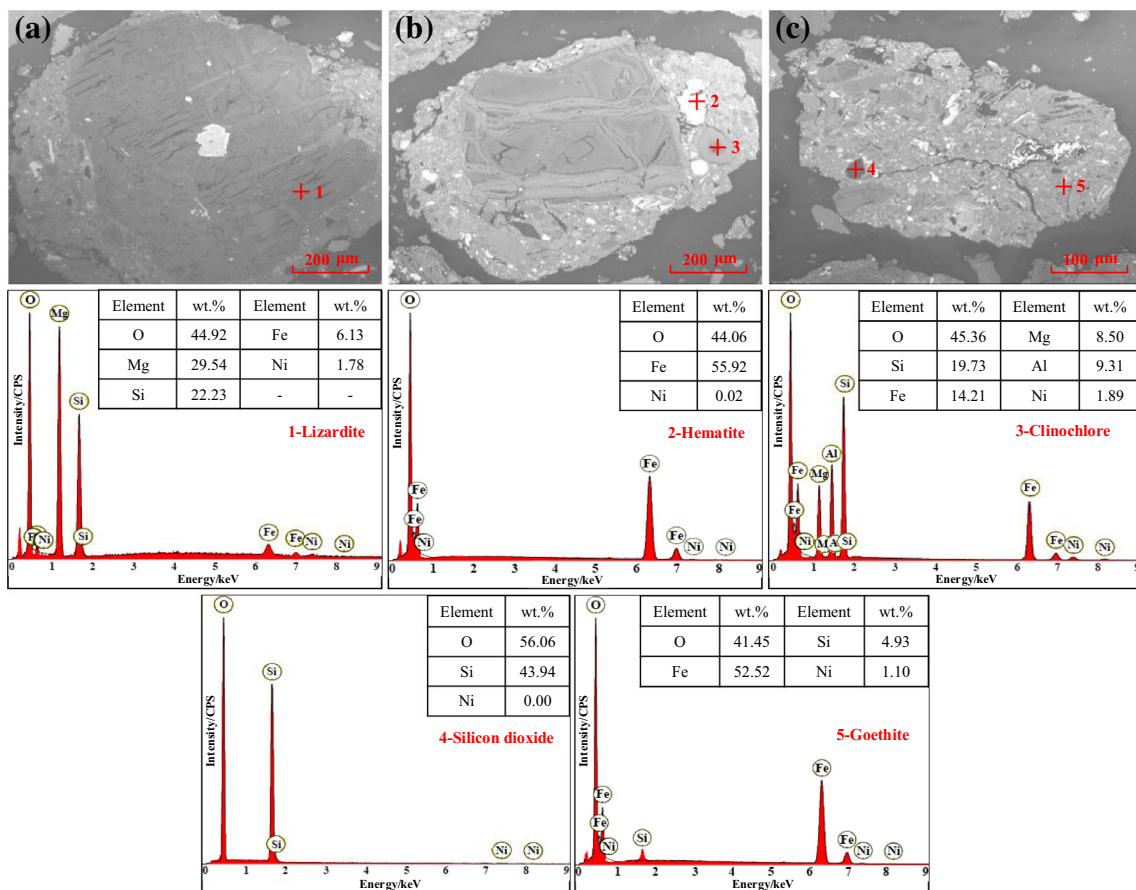


Fig. 2 SEM–EDS patterns of nickel laterite

**Table 2** Proximate and fusibility analyses of reductant

Proximate analysis/%				Ash fusibility analysis/°C			
M <sub>ad</sub>	V <sub>ad</sub>	A <sub>ad</sub>	FC <sub>ad</sub>	DT	ST	HT	FT
7.61	33.42	4.34	54.63	1290	1310	1320	1330

M<sub>ad</sub> Moisture; A<sub>ad</sub> ash; V<sub>ad</sub> volatile matter; FC<sub>ad</sub> fixed carbon; DT distortion temperature; ST softening temperature; HT hemispherical temperature; FT flow temperature

**Table 3** Chemical compositions of ash from reductant (wt.%)

TFe	SiO <sub>2</sub>	Al <sub>2</sub> O <sub>3</sub>	CaO	MgO	K <sub>2</sub> O	Na <sub>2</sub> O	P	S
4.84	24.42	6.68	33.64	2.30	0.14	1.20	0.07	12.67

### 2.1.3 Composite additive

The composite additive mainly comprising sodium humate, calcium carbonate and calcium fluoride with LOI of 27.88 wt.% was prepared in the form of powder less than 0.074 mm by Central South University in order to improve the recycling efficiency of Ni and Fe from nickel laterite by direct reduction and magnetic separation process.

### 2.1.4 Nucleating agent

Low-nickel concentrates (LNC) were applied as nucleating agent for further improving the growth of Ni–Fe fine particles in the process of direct reduction and magnetic separation, which were produced from the nickel laterite under the condition of C/Fe of 1.00 at reduction temperature of 1250 °C for 80 min followed by grinding fineness of 90% passing 0.074 mm and magnetic field intensity of 0.15 T, and their chemical compositions are presented in Table 4. The low-nickel iron-based alloy concentrates contain metals content of 72.43 wt.% with Ni grade of 4.65% and Fe/Ni of 14.58. Furthermore, the harmful elements involving S and P are very low. Hence, the used low-nickel concentrates can meet the requirement of nucleating agent.

## 2.2 Experimental methods

### 2.2.1 Improved direct reduction followed by magnetic separation at laboratory scale

Nickel laterite was first pre-treated by drying, crushing and sieving in order to yield a particle size below 0.5 mm (70% passing 0.074 mm) and was mixed sufficiently with a required ratio of low-nickel concentrates (0, 5%, 10%, 15%, 20%, 25%), composite additive (0, 2%, 3%, 5%, 7%)

**Table 4** Chemical compositions of low-nickel concentrates (wt.%)

Fe	Ni	SiO <sub>2</sub>	Al <sub>2</sub> O <sub>3</sub>	CaO	MgO	S	P
67.78	4.65	13.01	1.39	0.68	7.01	0.18	0.02

and suitable water. Then, the ore mixtures were made into a disk pelletizer with a diameter of 1000 mm, an incline angle of 47° to horizon and a speed of 38 r/min for pelletizing. Subsequently, the green balls sized between 12 and 16 mm were dried at 105 °C to a constant mass.

At each direct reduction experiment, about 50 g dried pellets were picked and mixed with a required proportion of soft coal (C/Fe of 0.25, 0.50, 0.75, 1.00, 1.50, 2.00, 2.50), and then charged into a corundum crucible with an inner diameter of 70 mm and height of 120 mm. Subsequently, the crucible was put into a muffle furnace when the target temperature (1100, 1150, 1200, 1250 and 1300 °C) was reached, and the reduction tests were conducted for a given period of time (40, 60, 80, and 100 min). After each reduction experiment was finished, the crucible was taken out rapidly and cooled down to room temperature under the protection of Ar gas. The cooled pellets separated from coals were then crushed to a size below 1 mm and mixed adequately for subsequent beneficiation process.

About 20 g samples were fine ground to a size of 100% passing 74 μm in a wet ball mill (RK/ZQM φ160 mm × 60 mm) with fixed slurry density of 50%. Subsequently, the mixed slurry was put into a Davis tube (CRIMM DCCXG φ50 mm) for magnetic separation of Ni–Fe concentrates from tailings at magnetic field intensity of 0.1 T for 10 min. The wet concentrates and tailings were both filtered and dried at 80 °C in a vacuum oven for 150 min for subsequent weighing and chemical analysis.

### 2.2.2 Grain growth kinetics

In the process of direct reduction and magnetic separation for recycling nickel and iron from nickel laterite, it is essential to realize not only the reduction in nickel(iron)-bearing phases into metallic states but also the growth of fine Ni–Fe alloy particles, in order to satisfy the subsequent magnetic separation process. In this study, a classical kinetic model of grain growth built by Sellars was employed to reveal the growth behavior of Ni–Fe alloy particles during the direct reduction in nickel laterite under the following conditions including (1) in absence of low-nickel concentrates and composite additive and (2) addition of 20% low-nickel concentrates and no composite additive. Based on the Sellars kinetic model of grain growth, the

growth rate of Ni–Fe alloy particles can be expressed by Eq. (1) [31]:

$$D^n - D_0^n = k_0 t \exp\left(-\frac{Q}{RT}\right) = kt \quad (1)$$

where  $D$  is the average size of Ni–Fe alloy particles at time  $t$ ,  $\mu\text{m}$ ;  $D_0$  is the average size of Ni–Fe alloy particles at initial time,  $\mu\text{m}$ ;  $n$  is a growth index of Ni–Fe alloy particles;  $k_0$  is the Boltzmann constant, J/K;  $t$  is the reduction duration, min;  $Q$  is the apparent activation energy of growth for Ni–Fe alloy particles, kJ/mol;  $R$  is a gas constant, J/mol;  $T$  is reduction temperature, K; and  $k$  is a constant of grain growth rate affected by diffusion,  $(\mu\text{m})^n/\text{min}$ , and  $k = k_0 \exp(-Q/(RT))$ .

Commonly, for the reduction stage in the direct reduction and magnetic separation process,  $D \gg D_0$ . Hence, Eq. (1) can be simplified as Eq. (2):

$$D^n = k_0 t \exp\left(-\frac{Q}{RT}\right) = kt \quad (2)$$

To further take the logarithm of Eq. (2), Eq. (3) can be obtained:

$$n \ln D = \ln k + \ln t \quad (3)$$

As shown in Eq. (3),  $\ln D$  presents a linear relationship with  $\ln t$  under a fixed reduction temperature and  $1/n$  is the slope, which can be used to calculate the growth index of Ni–Fe alloy particles.

Furthermore, for the same reduction time at different reduction temperatures in the direct reduction process, Eq. (2) can also be simplified as Eq. (4):

$$n \ln D = \ln k_0 t - \frac{Q}{RT} \quad (4)$$

As presented in Eq. (4),  $t$  is a constant and  $\ln D$  shows a linear relationship with  $1/T$ , and  $-Q/(nR)$  is the slope, which can be used to calculate the apparent activation energy of growth for Ni–Fe alloy particles.

The grade of nickel and iron in the raw ore, reduced pellets and magnetic concentrates was detected according to the Chinese standards GB/T 31924-2015 and GB/T 6730.5-2007, respectively. Furthermore, the corresponding recovery rates of nickel and iron are expressed as Eq. (5):

$$\omega = m/m_0 \times \varphi/\delta \times 100\% \quad (5)$$

where  $\omega$  is the recovery of nickel or iron, %;  $m_0$  is the mass of the reduced pellets, g;  $m$  is the mass of concentrates, g;  $\delta$  is the nickel or iron grade of reduced pellets, wt.%; and  $\varphi$  is the nickel or iron grade of concentrates, wt.%.

## 2.2.3 Characterization methodology

The X-ray diffraction instrument (SIMENS D500) combined with MDI Jade 6.0 software was applied to disclose the phase composition of samples. The Leica optical microscope (DM RXP), scanning electron microscope and energy dispersive spectrometer (Phenom ProX) were employed to reveal the microstructure of samples and micromorphology change of Ni–Fe alloy particles. Image-Pro Plus 6.0 was utilized to count the size of Ni–Fe particles in the reduced pellets.

## 3 Results and discussion

### 3.1 Improved reduction for recycling of Ni and Fe

The stage of reduction as the primary procedure of direct reduction and magnetic separation process is crucial for the recovery of Ni and Fe from nickel laterite. Hence, the effect of reduction parameters on recycling efficiency of Ni and Fe was explored systematically.

#### 3.1.1 Effect of proportion of low-nickel concentrates

The effect of low-nickel concentrates on recycling efficiency of Ni and Fe was conducted and the results are presented in Fig. 3. It shows that with an increase in proportion of low-nickel concentrates from 0 to 20%, the grade of Ni and Fe was elevated slightly from 4.11% and 56.36% to 4.54% and 56.88%, while the recovery of Ni and Fe was increased significantly from 57.81% and 62.68% to 81.43% and 86.43%, respectively. When the proportion of low-nickel concentrates continues to increase to 25%, the

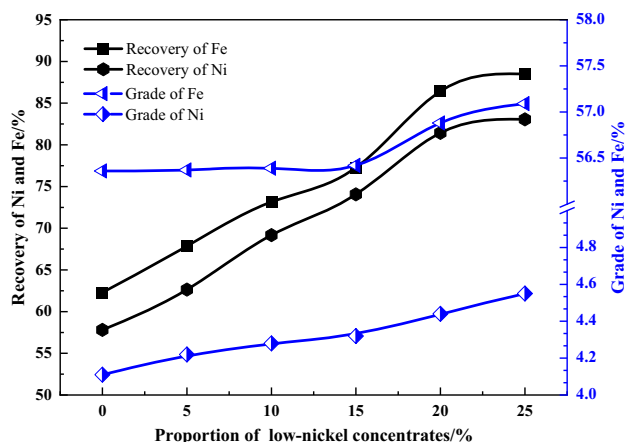
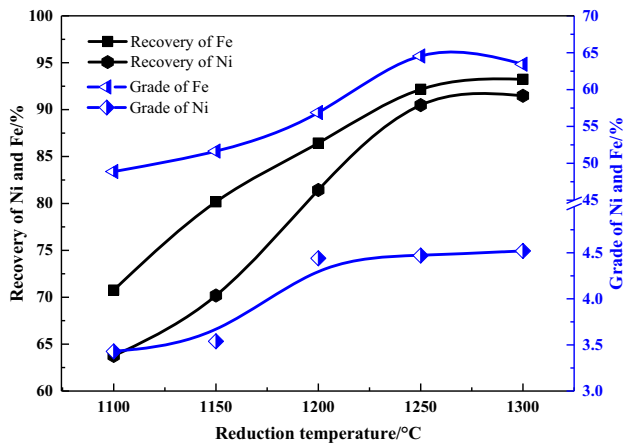


Fig. 3 Effect of low-nickel concentrates on recycling efficiency of Ni and Fe (reduction at 1200 °C for 80 min with composite additives of 3% and C/Fe of 2.00)



**Fig. 4** Effect of reduction temperature on recycling efficiency of Ni and Fe (reduction for 80 min with low-nickel concentrates of 20%, composite additives of 3% and C/Fe of 2.00)

recovery and grade of Ni and Fe roughly keep a constant tendency. It indicates that the suitable addition of low-nickel concentrates is beneficial to improve the recycling efficiency of Ni and Fe, which plays an important role in the direct reduction and magnetic separation process. However, excessive proportion of low-nickel concentrates may bring an adverse effect; compared with the Fe/Ni of 12.6 in the raw ore, the low-nickel concentrates have a higher Fe/Ni of 14.7, resulting in a lower Ni grade of magnetic concentrates. Therefore, the additional proportion of low-nickel concentrates is recommended to be 20%.

### 3.1.2 Effect of reduction temperature

The reduction temperature causes a significant effect on recycling efficiency of Ni and Fe, and the results are shown in Fig. 4. It indicates that as the reduction temperature increases from 1100 to 1250 °C, the grade of Ni and Fe in the magnetic concentrates was improved obviously from 3.42% and 48.89% to 4.47% and 64.55% with corresponding recovery of Ni and Fe from 63.74% and 70.76% to 90.48% and 92.17%, respectively. Afterward, the grade and recovery of Ni and Fe maintain constant with further raising the temperature. It implied that suitable temperature is favorable to the recycling efficiency of Ni and Fe by means of the improvement of mass transfer effect and the further acceleration of aggregation and growth for Ni-Fe fine particles, resulting in a better efficiency of subsequent magnetic separation. Hence, the optimum reduction temperature is recommended as 1250 °C.

### 3.1.3 Effect of reduction time

The effect of reduction time on recycling efficiency of Ni and Fe is shown in Fig. 5, which indicates that with the

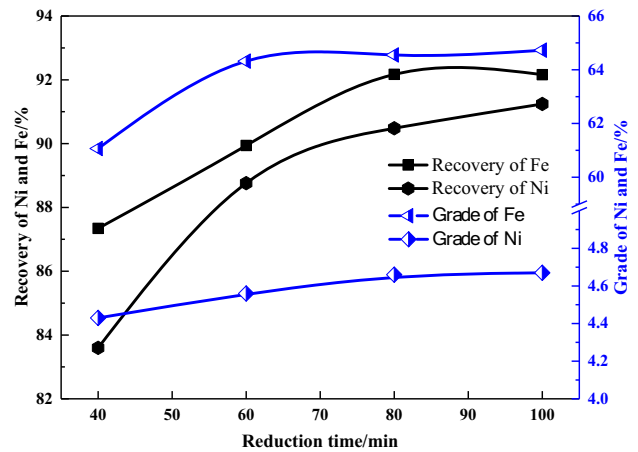


**Fig. 5** Effect of reduction time on recycling efficiency of Ni and Fe (reduction at 1250 °C with low-nickel concentrates of 20%, composite additives of 3% and C/Fe of 2.00)

extension of reduction time from 40 to 80 min, various indicators prominently ascend firstly and then change slightly. It is implied that sufficient time is essential to the reduction in nickel laterite and the increase in Ni-Fe grain size. Taking the energy consumption into consideration, the reduction time of 80 min should be reasonable.

### 3.1.4 Effect of dosage of composite additive

Commonly, the addition of suitable additive is an effective method to improve the recycling efficiency of Ni and Fe from nickel laterite in the direct reduction and magnetic separation process, which can be proved in Fig. 6. Compared with the low grade of 3.25% Ni and 50.16% Fe in the magnetic concentrates with poor corresponding recovery of 60.23% Ni and 74.62% Fe in absence of additive, the preferable magnetic concentrates can be obtained with

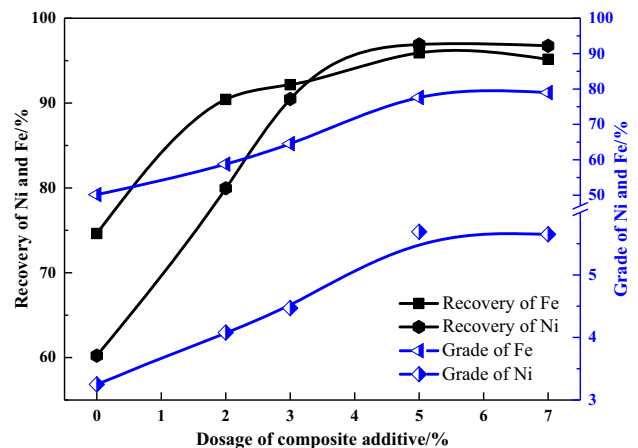


**Fig. 6** Effect of composite additive on recycling efficiency of Ni and Fe (reduction at 1250 °C for 80 min with low-nickel concentrates of 20% and C/Fe of 2.00)

5.69% Ni and 77.60% Fe with corresponding recovery rates of 96.91% and 95.92%, respectively, as the dosage of composite additives increases to 5%. The beneficial effects of composite additives include not only the acceleration of liquid phase generation to improve the mass diffusion but also the decrease in activation energy for the growth of fine Ni–Fe grains. However, excessive addition of additives will increase the cost of production but no further obvious effects. Hence, a dosage of composite additive addition is recommended as 5%, which is much fewer in comparison to that used in conventional direct reduction and magnetic separation processes in absence of low-nickel concentrates [32].

### 3.1.5 Effect of C/Fe mass ratio

Undoubtedly, the suitable reduction atmosphere is essential to recycle the nickel and iron from nickel laterite in the direct reduction and magnetic separation process. The effect of C/Fe mass ratio on recycling efficiency of Ni and Fe was investigated and the results are presented in Fig. 7. It is implied that with an increase in C/Fe from 0.25 to 2.00, the recovery of Ni and Fe shows an obvious tendency of increase from 81.84% and 78.32% to 96.90% and 95.92%, respectively, while the grade of Ni increases first to 6.44% and then decreases to 5.69% due to the fact that the continuous increase in Fe grade will dilute the Ni grade in the crude alloy. When the C/Fe is over 2.00, each index nearly keeps constant. With consideration of high-nickel concentrates as raw feeds applied into RKEF process, the recovery of Ni and Fe is regarded as the main parameter for reference. Hence, the C/Fe of 2.00 is recommended.

The magnetic concentrates were obtained under the suggested conditions as follows: reduction at 1250 °C for 80 min with C/Fe mass ratio of 2.00, low-nickel

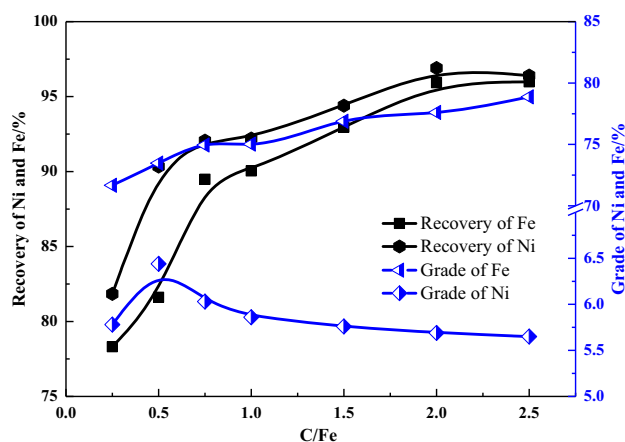


**Fig. 7** Effect of C/Fe mass ratio on recycling efficiency of Ni and Fe (reduction at 1250 °C for 80 min with low-nickel concentrates of 20% and composite additives of 5%)

concentrates of 20% and composite additives of 5%. The chemical compositions of magnetic concentrates and tailings are listed in Table 5. It indicates that the concentrates contain 6.44% Ni and 82.48% Fe and possess nearly 89% metals content, which are the superior crude alloy powder with low sulfur and phosphorus contents. Furthermore, tailings contain high contents of SiO<sub>2</sub> and CaO with a small quantity of harmful elements, which has a similar composition with that of serpentine and can be used in sintering as a kind of flux. Hence, the application of tailings into sintering can be taken into consideration.

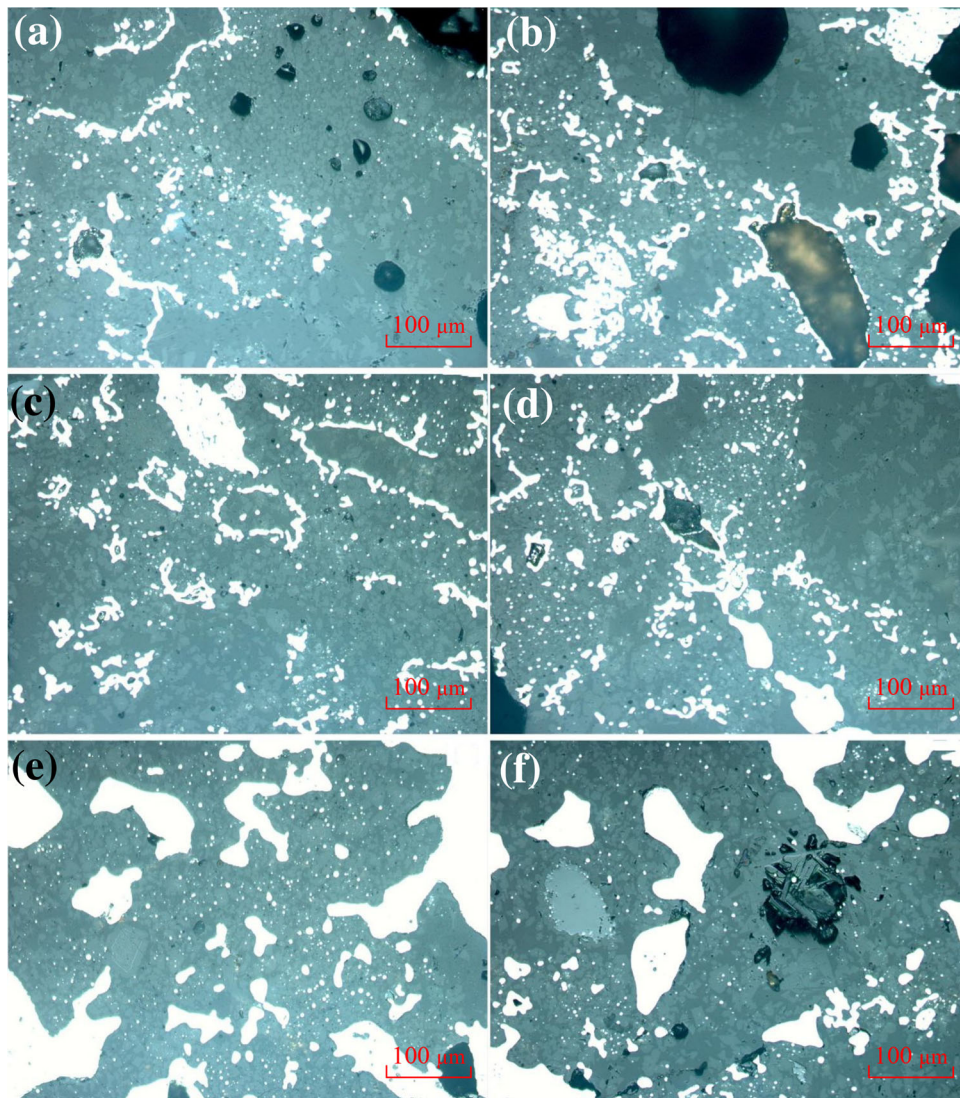
### 3.2 Growth mechanism of Ni–Fe alloy particles

The growth level of Ni–Fe alloy particles during the direct reduction stage is of great importance for the recovery of Ni and Fe in the direct reduction and magnetic separation process. Commonly, the bigger size of Ni–Fe alloy particles is preferable for their separation efficiency from gangue phases at subsequent stage of magnetic separation. The effect of dosage of low-nickel concentrates on microstructure of reduced pellets was analyzed, and the results are illustrated in Fig. 8, where white color represents alloy. It shows that in the absence of low-nickel concentrates, the Ni–Fe particles show a dispersive distribution with tiny dissemination, which causes an incomplete degree of dissociation from gangue phases and poor separation efficiency, resulting in a low recovery rate of nickel and iron. However, with the increase in proportion of low-nickel concentrates from 0 to 25%, the fine Ni–Fe particles gradually aggregated and enlarged with the improved shape from banded structure to blocky structure, which favors magnetic separation.

Furthermore, in order to reveal the growth mechanism of Ni–Fe particles by addition of nickel concentrates, the growth kinetics of Ni–Fe particles were further clarified. The effects of reduction temperature and time on the average size of the Ni–Fe alloy particles in the reduced pellets are presented in Fig. 9a, b, respectively. The results show that the elevated temperature from 1000 to 1250 °C and the prolonged time from 0 to 80 min can both play effective roles in the growth of Ni–Fe alloy particles in the reduction process, because the suitable increases in reduction temperature and time are beneficial to the reduction in Ni(Fe)-bearing phases and the migration, aggregation and growth of fine Ni–Fe alloy particles. In addition, compared with single nickel laterite in the absence of low-nickel concentrates, the reduction temperature and time both present a more significant effect on the average size of Ni–Fe alloy in the reduced pellets by addition of 20% low-nickel concentrates. When a reduction test at 1250 °C for 80 min with C/Fe of 2.00 was performed, the average sizes of Ni–Fe alloy particles have

**Table 5** Chemical compositions of magnetic concentrates and tailings (wt.%)

Element	TFe	TNi	SiO <sub>2</sub>	Al <sub>2</sub> O <sub>3</sub>	CaO	MgO	C	S	P
Concentrates	82.48	6.44	3.11	0.71	0.72	3.42	0.03	0.21	0.03
Tailings	8.30	0.32	45.10	2.48	5.26	36.58	0.04	0.09	0.02

**Fig. 8** Effect of dosage of low-nickel concentrates on microstructure of reduced pellets (reduction roasting at 1250 °C for 80 min with C/Fe of 2.00). **a** 0; **b** 5%; **c** 10%; **d** 15%; **e** 20%; **f** 25%

reached 21  $\mu\text{m}$  by addition of 20% low-nickel concentrates, while that for single nickel laterite is only less than 10  $\mu\text{m}$ , which implied that the fine Ni–Fe alloy particles in the pellets of single nickel laterite are more difficult to grow.

Furthermore, the linear relationships of  $\ln D$  to  $\ln t$  and  $1/T$  for the growth performance of Ni–Fe alloy particles were analyzed with the assistance of Fig. 9a, b as well as

Eqs. (3) and (4), and the results are shown in Fig. 10 and Table 6. As can be seen from Fig. 10, the relationships of  $\ln D$  to  $\ln t$  and  $1/T$  both show a good linearity with high correlation coefficient ( $R^2$ ) values of not less than 0.94, which indicates that the results of linear fitting are acceptable. In addition, as known from the growth performances of Ni–Fe alloy particles in the procedure of direct reduction listed in Table 6, the Ni–Fe alloy particles



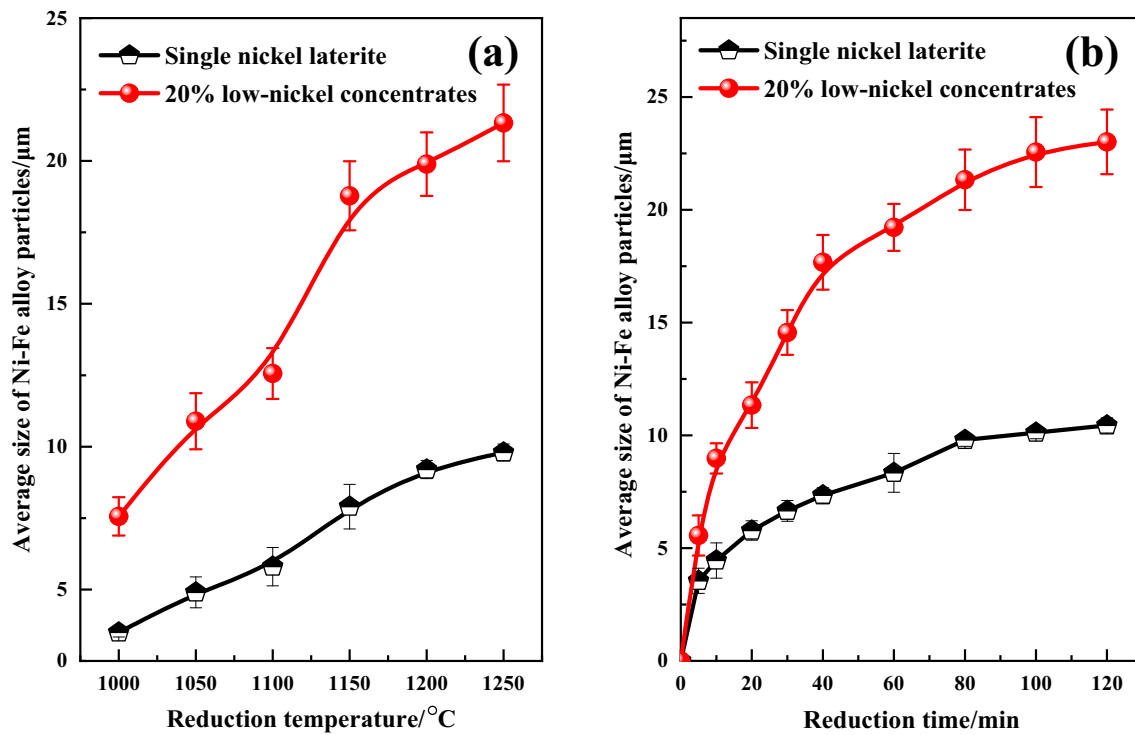


**Fig. 9** Effect of reduction temperature and time on average size of Ni-Fe alloy particles in reduced pellets. **a** Reduction for 80 min with C/Fe of 2.00; **b** reduction at 1250 °C with C/Fe of 2.00

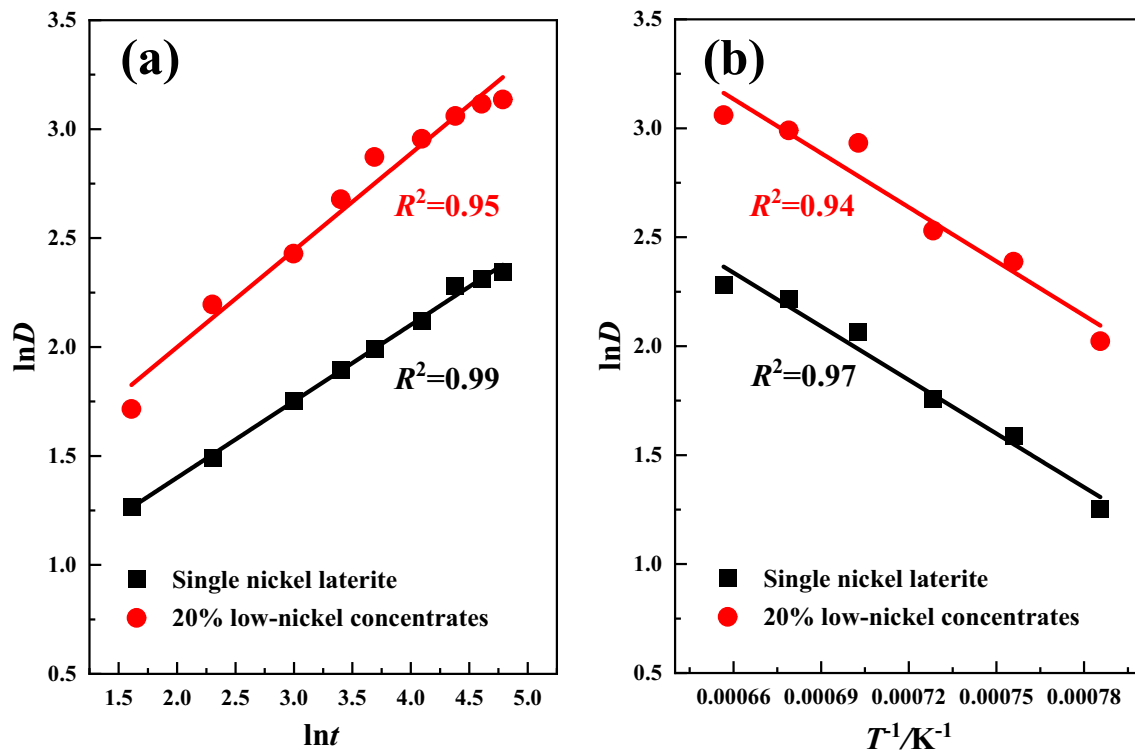


**Fig. 10** Linear relationships of  $\ln D$  to  $\ln t$  (a) and  $1/T$  (b)

**Table 6** Growth performances of Ni–Fe alloy particles in procedure of direct reduction

Scheme	<i>n</i>	<i>k</i> / ( $\mu\text{m}^n \text{min}^{-1}$ )	Grain growth relation	<i>Q</i> / ( $\text{kJ mol}^{-1}$ )
1	3	1.224	$\exp(0.351\ln t + 0.699)$	197.10
2	3	1.283	$\exp(0.444\ln t + 1.111)$	154.81

Scheme 1 Single nickel laterite; scheme 2 addition of 20% low-nickel concentrates

in the two types of reduction schemes have a same growth index of 3. For the scheme of single nickel laterite, the growth rate constant of Ni–Fe alloy particles is  $1.224 \mu\text{m}^3/\text{min}$  with grain growth relation of  $\exp(0.351\ln t + 0.699)$ , while for the scheme of 20% low-nickel concentrates, it is  $1.283 \mu\text{m}^3/\text{min}$  with grain growth relation of  $\exp(0.444\ln t + 1.111)$ , which implies that suitable addition of low-nickel concentrates has a significant acceleration for the growth of the alloy particles. Besides, the activation energy for growth of Ni–Fe alloy particles is as high as 197.10 kJ/mol in the scheme of single nickel laterite, while it decreases as low as 154.81 kJ/mol in the scheme of 20% low-nickel concentrates, which further indicates that low-nickel concentrates can reduce the degree of difficulty for the growth of Ni–Fe alloy particles.

The reasons are that the low-nickel concentrates as a nucleating additive are beneficial to decrease the grain boundary surface energy and break through the nucleation barrier for improving the migration and growth of fine Ni–Fe alloy particles. Hence, with the positive effect of low-nickel concentrates, the average size of Ni–Fe alloy particles shows an obvious increase.

### 3.3 Characteristics of phases transformation and elements distribution

According to previous reports [29], for the single nickel laterite subjected to the direct reduction process, its mineral phases mainly consist of crude Ni–Fe alloy and slag phases including forsterite ( $\text{Mg}_2\text{SiO}_4$ ), hortonolite ( $(\text{Mg}, \text{Fe})_2\text{SiO}_4$ ) and enstatite ( $(\text{Mg}, \text{Fe})_2\text{Si}_2\text{O}_6$ ) characterized by high melting point. As a result, the high temperature is always needed to realize the growth of Ni–Fe alloy particles, which is easy to cause the ringing formation of rotary kiln and undoubtedly increase the energy consumption of production. Hence, the suitable additive was employed in the direct reduction and magnetic separation process to accelerate the generation of low-melting-point mineral phases such as melilite ( $\text{Ca}_2\text{MgSi}_2\text{O}_7$ ) and tremolite ( $\text{Ca}_2\text{Mg}_5[\text{Si}_8\text{O}_{22}]\text{F}_2$ ) in the pellets as illustrated in Fig. 11. Furthermore, as can be seen from Fig. 11, the diffraction

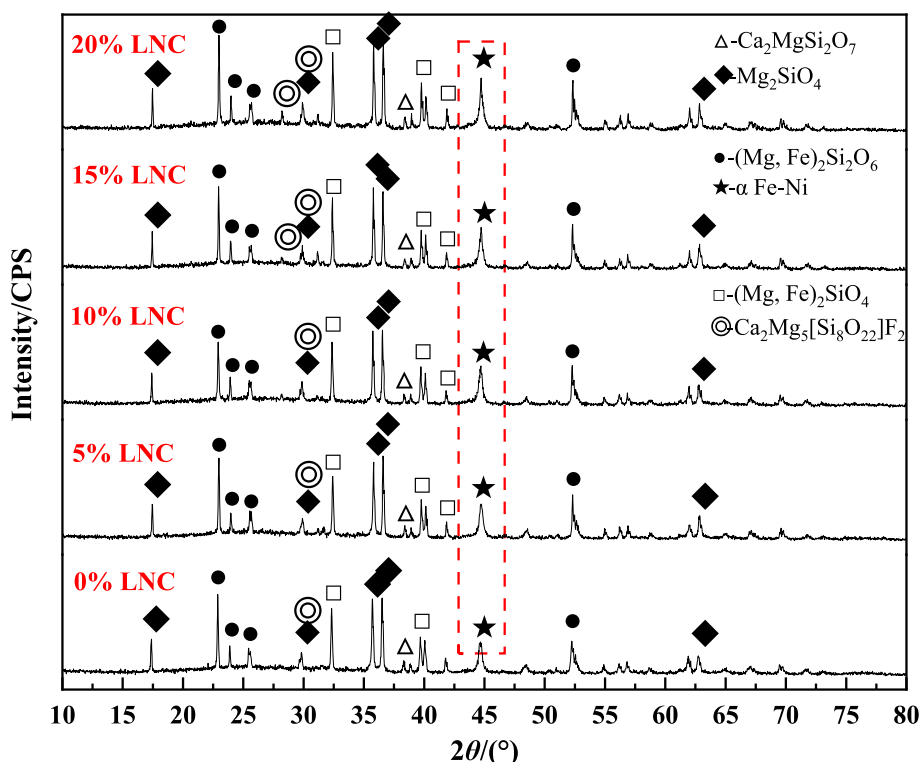


**Fig. 11** XRD pattern of reduced pellets with different dosages of low-nickel concentrates (reduction at 1250 °C for 80 min with composite additive of 5% and C/Fe of 2.00)

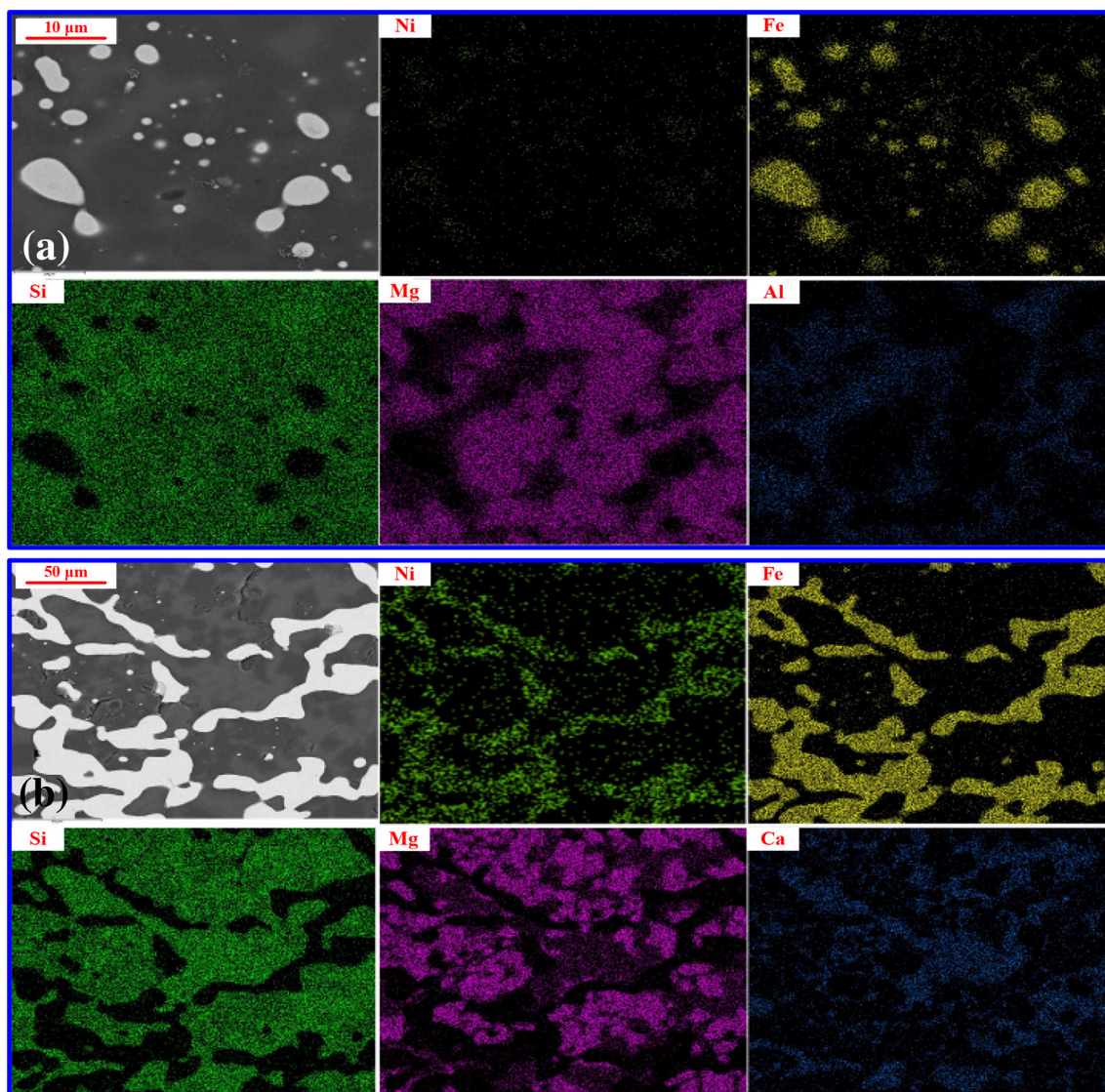


**Fig. 12** Microstructure and corresponding elemental scanning images of reduced nickel laterite pellets. **a** Reduction at 1250 °C for 80 min with C/Fe of 2.00; **b** reduction at 1250 °C for 80 min with low-nickel concentrates of 20% and C/Fe of 2.00

peak intensity of Ni–Fe gradually increases with the increase in low-nickel concentrates from 0 to 20%. It is because the addition of low-nickel concentrates can not only increase the content of Ni and Fe in the reduced pellets, but also accelerate the growth of Ni–Fe alloy particles in an improved alloy crystal and low lattice imperfection, which further presents the beneficial effects on the growth of Ni–Fe alloy particles.

The microstructure and corresponding elemental scanning images of the reduced nickel laterite pellets are presented in Fig. 12. As can be seen from Fig. 12a, for the reduction in single nickel laterite, a great mass of iron element is enriched in the alloy phase, and a good separation from slag phase is exhibited, while the nickel element has a dispersive distribution with a poor consistency

to the iron element. It indicates that the nickel has not completely migrated into the iron-based alloy, which may result in a low recovery of Ni at the subsequent magnetic separation process. However, in the presence of low-nickel concentrates in the nickel laterite pellets, the vast majority of Ni element shows a preferable distribution with Fe element and they are both prone to enrich in the alloy phase, which is illustrated in Fig. 12b. Furthermore, compared with the reduction in single nickel laterite, the addition of low-nickel concentrates will not only evidently increase the particle size of the metallic phase, but also bring a more obvious dividing line between the metallic phase and gangue phase, which is conducive to a satisfied liberation of the metallic phase from the gangue phase in the subsequent procedure of fine grinding, in order to meet

the requirement of magnetic separation for the recycling of Ni and Fe, and significantly improve the recovery of Ni and Fe from nickel laterite.

## 4 Conclusions

1. The preferable Ni–Fe alloy concentrates with 6.44% Ni and 82.48% Fe can be prepared by reduction at 1250 °C for 80 min with low-nickel concentrates of 20%, composite additive of 5% and C/Fe of 2.00 followed by subsequent magnetic separation. The corresponding recovery of Ni and Fe was 96.90% and 95.92%, respectively.
2. The low-nickel concentrates with 4.65% Ni and 67.68% Fe, produced from direct reduction and magnetic separation process, as a nucleating agent can obviously reduce the activation energy for growth of Ni–Fe alloy particles during the improved direct reduction process from 197.10 to 154.81 kJ/mol with the addition of 20%, resulting in an increase in size for Ni–Fe particles in the pellets from less than 10 μm to more than 20 μm.

**Acknowledgements** This work was financially supported by the Youth Natural Science Foundation of China (No. 51904347), the National Natural Science Foundation of China (No. 51574281) and Innovation-driven Project of Guangxi Zhuang Autonomous Region (No. AA18242003). The authors would like to thank the Fundamental Research Funds for the Central Universities of Central South University, which supplied us the facilities and funds to fulfill the experiments.

## References

- [1] B.K. Reck, V.S. Rotter, *J. Ind. Ecol.* 16 (2012) 518–528.
- [2] N.R. Baddoo, *J. Constr. Steel Res.* 64 (2008) 1199–1206.
- [3] D.Q. Zhu, H.Y. Tian, J. Pan, H. Liao, Z.Q. Guo, Y.X. Xue, *J. Iron Steel Res.* 32 (2020) 351–362.
- [4] D.Q. Zhu, Y. Cui, S. Hapugoda, K. Vining, J. Pan, *Trans. Nonferrous Met. Soc. China* 22 (2012) 907–916.
- [5] D.Q. Zhu, Y. Cui, K. Vining, S. Hapugoda, J. Douglas, J. Pan, G.L. Zheng, *Int. J. Miner. Process.* 106–109 (2012) 1–7.
- [6] W. Luo, Q.M. Feng, L.M. Ou, G.F. Zhang, Y.P. Lu, *Hydrometallurgy* 96 (2009) 171–175.
- [7] Y.Y. Zhang, K.K. Cui, J. Wang, X.F. Wang, J.M. Qie, Q.Y. Xu, T.H. Qi, *Powder Technol.* 376 (2020) 496–506.
- [8] A. Oxley, N. Barcza, *Miner. Eng.* 54 (2013) 2–13.
- [9] R.D. Laranjo, N.M. Anacleto, *J. Iron Steel Res. Int.* 25 (2018) 515–523.
- [10] J.H. Zhang, L.H. Gao, Z.J. He, X.M. Hou, W.L. Zhan, Q.H. Pang, *J. Mater. Res. Technol.* 9 (2020) 12223–12235.
- [11] X.D. Ma, Z.X. Cui, B.J. Zhao, *JOM* 68 (2016) 3006–3014.
- [12] R.J. Hundermark, L.R. Nelson, *JOM* 69 (2017) 335–342.
- [13] P. Liu, B.K. Li, S.C.P. Cheung, W.Y. Wu, *Appl. Therm. Eng.* 109 (2016) 542–559.
- [14] J.Z. Khoo, N. Haque, G. Woodbridge, R. McDonald, S. Bhattacharya, *J. Clean. Prod.* 142 (2017) 1765–1777.
- [15] W. Rong, B. Li, P. Liu, F. Qi, *Energy* 138 (2017) 942–953.
- [16] L.H. Gao, Z.G. Liu, Y.Z. Pan, Y. Ge, C. Feng, M.S. Chu, J. Tang, *Min. Metall. Explor.* 36 (2019) 375–384.
- [17] L.W. Wang, X.M. Lü, M. Liu, Z.X. You, X.W. Lü, C.G. Bai, *Int. J. Miner. Metall. Mater.* 25 (2017) 744–751.
- [18] Y.J. Li, Y.S. Sun, Y.X. Han, P. Gao, *Trans. Nonferrous Met. Soc. China* 23 (2013) 3428–3433.
- [19] D.Q. Zhu, L.T. Pan, Z.Q. Guo, J. Pan, F. Zhang, *Adv. Powder Technol.* 30 (2019) 451–460.
- [20] X.H. Tang, R.Z. Liu, L. Yao, Z.J. Ji, Y.T. Zhang, S.Q. Li, *Int. J. Miner. Metall. Mater.* 21 (2014) 955–961.
- [21] S. Pintowantoro, F. Abdul, *Mater. Trans.* 60 (2019) 2245–2254.
- [22] X. Jiang, L. He, L. Wang, D.W. Xiang, H.W. An, F.M. Shen, *Metall. Mater. Trans. B* 51 (2020) 2653–2662.
- [23] S. Yuan, W.T. Zhou, Y.J. Li, Y.X. Han, *Trans. Nonferrous Met. Soc. China* 30 (2020) 812–822.
- [24] H. Tsuji, *ISIJ Int.* 52 (2012) 1000–1009.
- [25] Y. Kobayashi, H. Todoroki, H. Tsuji, *ISIJ Int.* 51 (2011) 35–40.
- [26] Y.F. Chen, X.M. Lv, Z.D. Pang, X.W. Lv, *J. Iron Steel Res. Int.* 27 (2020) 1400–1406.
- [27] J.C. Dong, Y.G. Wei, S.W. Zhou, B. Li, Y.D. Yang, A. Mclean, *JOM* 70 (2018) 2365–2377.
- [28] Z.Q. Guo, J. Pan, D.Q. Zhu, F. Zhang, *JOM* 70 (2018) 150–154.
- [29] H.Y. Tian, J. Pan, D.Q. Zhu, C.C. Yang, Z.Q. Guo, Y.X. Xue, *J. Mater. Res. Technol.* 9 (2020) 2578–2589.
- [30] M.J. Rao, G.H. Li, T. Jiang, J. Luo, Y.B. Zhang, X.H. Fan, *JOM* 65 (2013) 1573–1583.
- [31] C.M. Sellars, J.A. Whiteman, *Met. Sci.* 13 (1979) 187–194.
- [32] S. Yu, Z. Tao, L.X. Du, *Hot Work. Technol.* 49 (2020) No. 6, 121–123.